Molecular Therapy
Methods & Clinical Development
Original Article

Optimal different adeno-associated virus capsid/promoter combinations to target specific cell types in the common marmoset cerebral cortex

Yasunori Matsuzaki,[1,2] Yuuki Fukai,[1] Ayumu Konno,[1,2] and Hirokazu Hirai[1,2]

[1]Department of Neurophysiology & Neural Repair, Gunma University Graduate School of Medicine, Maebashi, Gunma 371-8511, Japan; [2]Viral Vector Core, Gunma University, Initiative for Advanced Research, Maebashi, Gunma 371-8511, Japan

To achieve cell-type-specific gene expression, using target cell-type-tropic different adeno-associated virus (AAV) capsids is advantageous. However, their tropism across brain cell types in nonhuman primates has not been fully elucidated. We assessed the tropism of nine AAV serotype capsids (AAV1, 2, 5, 6, 7, 8, 9, rh10, and DJ) expressing EGFP by chicken β-actin hybrid (CBh) promoter in marmoset cerebral cortical cells. All nine AAV capsid vectors, especially AAV9 and AAVrh10, caused highly neuron-selective EGFP expression. Some AAV capsids, including AAV5, induced EGFP expression to a lesser extent in oligodendrocytes. Different ubiquitous cytomegalovirus (CMV) and CMV early enhancer/chicken β-actin (CAG) promoters exhibited similar neuron-predominant transgene expression. Conversely, all nine AAV capsid vectors with the astrocyte-specific hGFA(ABC1D) promoter selectively expressed EGFP in astrocytes, except AAV5, which modestly expressed EGFP in oligodendrocytes. Oligodendrocyte-specific mouse myelin basic protein (mMBP) promoter in AAV5 vectors expressed EGFP in oligodendrocytes specifically and efficiently. The following are optimal combinations of capsids and promoters for cell-type-specific expression: AAV9 or AAVrh10 and ubiquitous CBh or CMV promoter for neuron-specific transgene expression, AAV2 or AAV7 and hGFA(ABC1D) promoters for astrocyte-specific transgene expression, and AAV5 and mMBP promoters for oligodendrocyte-specific transgene expression.

INTRODUCTION

The brain is an organ in which an extremely large number of cells, including neurons, astrocytes, oligodendrocytes, and microglia, extend their processes and become intertwined. Recent studies have shown that specific cell types play important roles in the onset and progression of brain diseases, including oligodendrocytes in multiple sclerosis,[1,2] microglia in Alzheimer disease,[3,4] and astrocytes and microglia in stroke.[5,6] For these brain diseases, delivering and expressing genes to specific cell types involved in the pathogenesis may allow the elucidation of the underlying molecular mechanisms and development of therapeutic interventions. However, the unintended expression of a gene in non-target cell types can cause non-specific effects, which makes interpretation difficult, and in the case of gene therapy, potentially leads to adverse events.

To express a gene specifically and efficiently in the target cell type, the combination of a target cell-tropic capsid and a target cell-selective promoter is crucial. Although the tropism of different adeno-associated virus (AAV) vector serotype capsids has been studied in rodents,[7–11] there are only a few studies in non-human primates,[11–13] probably due to the limited number of animals available. Masamizu et al. injected AAV8 or AAV9 expressing EGFP under the control of the ubiquitous cytomegalovirus (CMV) promoter into the cerebral cortex of marmosets and found transgene expression almost exclusively in neurons,[12,13] whereas Watakabe et al. observed glial cell-dominant transgene (humanized *Renilla reniformis* GFP [hrGFP]) expression in the marmoset cortex that was injected with AAV1, 5, 8, or 9 carrying the CMV promoter.[11] Glial cell-dominant gene expression in the marmoset cortex by AAV vectors may be due to tissue damage and subsequent inflammation caused by high-dose AAV injection and the toxicity of high levels of hrGFP expression, as Watakabe et al. observed neuronal loss and glial infiltration at the AAV injection sites.[11] Therefore, the tropism of different AAV serotypes in the marmoset cortex has not yet been fully elucidated.

In the present study, we determined the dose of EGFP-expressing AAV vectors that did not cause apparent tissue damage after intraparenchymal AAV injection. Subsequently, nine different serotype capsid vectors (AAV1, 2, 5, 6, 7, 8, 9, rh10, and DJ), which expressed EGFP by the ubiquitous 0.8-kb chicken β-actin hybrid (CBh) promoter,[14] at the dose decided upon were injected to explore the tropism of those capsids to distinct brain cell types in marmosets. In addition, we examined whether the combination of target cell-tropic capsids with appropriate promoters enabled target cell-specific gene expression in the marmoset brain. Our results, which reveal the

Received 11 May 2024; accepted 10 September 2024;
https://doi.org/10.1016/j.omtm.2024.101337.

Correspondence: Hirokazu Hirai, Department of Neurophysiology and Neural Repair, Gunma University Graduate School of Medicine, Maebashi, Gunma 371-8511, Japan.
E-mail: hirai@gunma-u.ac.jp

Table 1. Marmoset profiles used for analysis of nine serotypes of AAV vectors expressing EGFP by the CBh, CMV, CAG, hGFA(ABC1D), or mMBP promoter

			AAV vector injection					Sacrifice		
ID	Name	Sex	Promoter	Titer (vg/serotype)	Volume (μL)	Old (y)	BW (g)	Incubation period (days)	BW (g)	Weight change (-fold)
H227	Shinobu	male	CBh	6.0×10^8	1	1.6	335	32	316	0.94
H231	Hamo	male	CBh	6.0×10^8	1	1.4	365	34	374	1.02
H232	Odoru	male	CBh	6.0×10^8	1	1.3	325	34	339	1.04
H257	Nishin	male	CBh, CMV	6.0×10^8	1	1.1	320	28	314	0.98
H259	Shirasu	female	CBh, CMV	6.0×10^8	1	1.1	338	29	340	1.01
H260	Hirame	male	CBh, CMV	6.0×10^8	1	1.1	384	29	391	1.02
H263	Maru	male	CBh, CMV	6.0×10^8	1	1.1	408	28	399	0.98
H149	Sango	female	CAG	6.0×10^8	1	5.8	340	28	357	1.05
H276	Yo	female	CAG	6.0×10^8	1	2.6	505	31	494	0.98
H309	Azami	female	CAG	6.0×10^8	1	1.7	488	29	487	1.00
H312	Hijiki	male	CAG	6.0×10^8	1	1.7	529	28	527	1.00
H256	Sawara	male	hGFA(ABC1D)	6.0×10^8	1	1.4	371	31	395	1.06
H268	Noko	female	hGFA(ABC1D)	6.0×10^8	1	1.2	316	29	328	1.04
H269	Take	male	hGFA(ABC1D)	6.0×10^8	1	1.2	344	33	401	1.17
H271	Aoba	male	hGFA(ABC1D)	6.0×10^8	1	1.2	333	29	344	1.03
H112	Azuki	female	mMBP	6.0×10^8	1	7.0	354	33	372	1.05
H262	Madoka	female	mMBP	6.0×10^8	1	2.3	450	30	467	1.04
H291	Kanro	male	mMBP	6.0×10^8	1	1.7	511	32	444	0.87
H295	Santa	male	mMBP	6.0×10^8	1	1.5	362	28	355	0.98

BW, body weight.

affinity of different AAV serotype capsids for primate cortical cell types and suitable capsid/promoter combinations for transgene expression in target cell types, may be useful for AAV capsid/promoter engineering in human AAV gene therapy.[15]

RESULTS

To compare the cellular tropism of the different AAV serotypes in the marmoset brain, we injected nine AAV serotypes (AAV1, 2, 5, 6, 7, 8, 9, rh10, and DJ) into the marmoset brain (see Table 1 for marmoset details). The AAV vectors were designed to express EGFP under the control of the constitutively active CBh promoter (Figures 1A and S1). Each AAV vector was injected at 10 locations in the marmoset cerebral cortex (Figure 1B). Because the injection of high-titer AAV causes inflammation and local tissue damage,[11] we first determined the optimal viral titer for the assessment. The marmoset cerebral cortex was injected with a triple dilution series of the AAV2 vector (1 μL/each point). EGFP expression and tissue conditions were examined 4 weeks after viral injection using fluorescent immunohistochemistry (fIHC). Low-magnification EGFP fluorescence images showed that the EGFP labeling area and fluorescence intensity were roughly proportional to the injected viral titer without affecting NeuN labeling (Figure S2A), indicating no neuronal loss over the range of AAV titers used. However, in the area that received the highest viral titer (2.0×10^9 viral genomes [vg]), microglia shape changed markedly with increased immunoreactivity, and microglial processes surrounded the neuronal cell bodies (Figure S2B). These results suggest a strong inflammatory response and tissue damage caused by the injection of high-dose AAV.

Since such pathological changes were not observed at AAV doses less than 6.0×10^8 vg (Figure S2C), we decided to use 6.0×10^8 vg of AAVs for the following experiments. Nine different serotype vectors were injected into the cerebral cortex of marmosets, which were sacrificed 4 weeks later, and the size of the GFP-expressing area and cell types were analyzed. The diameters of the GFP-fluorescent areas were measured from the cerebral surface to compare the strength of expression in each capsid (Figure 1C). The diameters of GFP fluorescence were not significantly different among the nine AAV serotypes (Figure 1D; $n = 3$–4 marmosets, $p = 0.146$ by the Kruskal-Wallis test); however, a tendency indicated that the GFP fluorescent areas upon AAV2 and AAV6 injection were smaller (Figures 1C and 1D).

Next, we prepared cerebral cortical sections to examine the cell types expressing GFP. The proportion of EGFP-expressing cell types (neurons, astrocytes, oligodendrocytes, and microglia) to the total number of EGFP-expressing cells was examined using fIHC. Because it was difficult to simultaneously immunolabel four different cell marker proteins in a single cerebral section, two serial sections were used: one immunostained with antibodies against NeuN (a neuron marker) and glial fibrillary acidic protein (GFAP) or S100β[16] (astrocyte

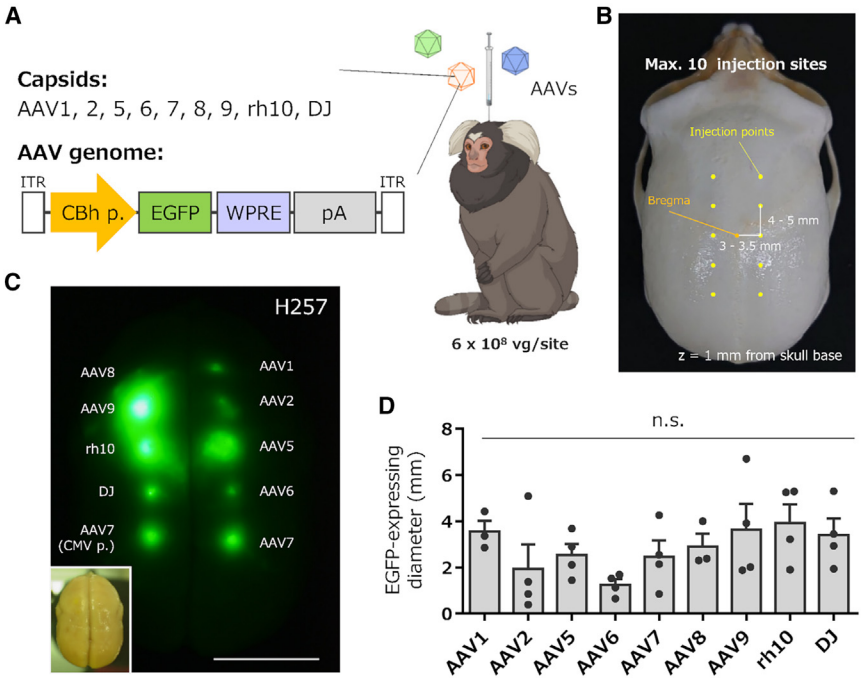

Figure 1. Comparison of expression levels of EGFP by injection of nine different serotype AAV vectors into the marmoset cortex

(A) Schema depicting injection of AAV vectors into a marmoset. Nine AAV capsid vectors expressing EGFP under the control of the CBh promoter were injected into the marmoset cerebral cortex. (B) The coordinate of the viral injection with reference to the bregma of the marmoset skull. (C) Example of EGFP fluorescence image of marmoset cortex 4 weeks after viral injection. The lower left inset is a bright-field brain image of a marmoset (animal ID: H257, see Table 1). Scale bar, 10 mm. (D) Graph showing the diameter of EGFP fluorescence on the cortex. Error bars indicate SEM, and dots in the graph indicate the respective values for each of the individual marmosets. No statistically significant differences were observed in the EGFP fluorescence diameters by a Kruskal-Wallis test with Dunn's post hoc test. n.s., not significant.

markers), and the other with antibodies against Olig2 (an oligodendrocyte marker) and Iba1 (a microglial marker) (Figure 2). The astrocyte marker GFAP is a membrane protein primarily expressed in astrocytic processes, and its expression levels increase depending on tissue damage and inflammation.[17,18] To measure the density of astrocytes in the intact cortex, we used S100β[16] instead of GFAP, as faint GFAP immunolabeling makes it difficult to identify astrocyte cell bodies.

We measured the percentage of cell types present in the intact cerebral cortex of marmosets using IHC. The cerebral cortex close to the injected sites (parietal lobe, Brodmann's area 7) contained 43.4% neurons, 11.7% astrocytes, 41.9% oligodendrocytes, and 3.0% microglia (counted area 0.67 mm^2, n = 3 marmosets analyzed; Figure S3). If AAV vectors infect and express a transgene in cortical cells in an unbiased manner, the proportion of cells expressing EGFP should follow the proportion that is endogenously present. However, the results showed that approximately 80%–95% of EGFP-expressing cells were neurons in all AAV serotypes examined (Figures 3A, 3B, and S4). Notably, nearly all EGFP-expressing cells were neurons when injected with AAV2, 6, 9, rh10, or DJ, whereas AAV5 showed a significantly lower ratio of neurons to total EGFP-expressing cells compared to neurotropic AAVrh10 (Figure 3B; n = 3–4 marmosets, $^*p < 0.05$, Kruskal-Wallis test with Dunn's post hoc test).

A minor fraction of EGFP-expressing cells were Olig2-labeled oligodendrocytes, in which AAV5 expressed EGFP at a relatively high proportion compared with many other serotypes (Figure 3C). However, the ratio of oligodendrocytes to all EGFP-expressing cells (approximately 20%) was much lower than the proportion of oligodendrocytes in the cells present in the cerebral cortex (42%). In contrast, none of the tested AAV serotypes expressed EGFP in the astrocytes or microglia (Figures 3D and 3E). Thus, all nine AAV serotype vectors tested preferentially expressed a transgene in neurons in the marmoset cerebral cortex, and AAV5 was unique in that it exhibited more transgene expression in oligodendrocytes than the other serotypes.

The lack of EGFP expression in astrocytes and microglia may be explained by the loss of CBh promoter activity in these cell types. Therefore, we performed similar experiments using AAV7 expressing EGFP under the control of another constitutive promoter, the CMV or CMV early enhancer/chicken β-actin (CAG) promoter[19,20] (Figure S1). We used the AAV7 capsid because, in our preliminary experiments using different AAV serotypes with astrocyte-specific GFAP promoters, AAV7 expressed a transgene in marmoset cortical astrocytes with high specificity, indicating that AAV7 is a suitable serotype to test whether the CBh, CMV, and CAG promoters function in astrocytes. When AAV7 carrying the CMV or CAG promoter was injected into the marmoset cortex, EGFP was expressed primarily in the neurons and moderately in the oligodendrocytes (Figures 4A–4C). None of the astrocytes expressed EGFP under the control of the CMV promoter. When using the CAG promoter, a small fraction of astrocytes expressed EGFP; however, the ratio of astrocytes to all EGFP-expressing cells (approximately 4%) was much lower than the proportion of astrocytes to cells present in the cerebral cortex (approximately 12%) (Figure 4D). No EGFP expression was observed in microglia, regardless of the promoter used (Figure 4E). Statistical analyses in Figures 4B–4E were performed using the Kruskal-Wallis test with Dunn's post hoc test (n = 4 marmosets).

To compare the tropism of different AAV serotypes for marmoset astrocytes, we injected nine serotype vectors expressing EGFP, using the astrocyte-specific human GFAP (hGFA(ABC1D)) promoter[21] (Figure 5A), into the marmoset cortex. Four weeks after viral injection,

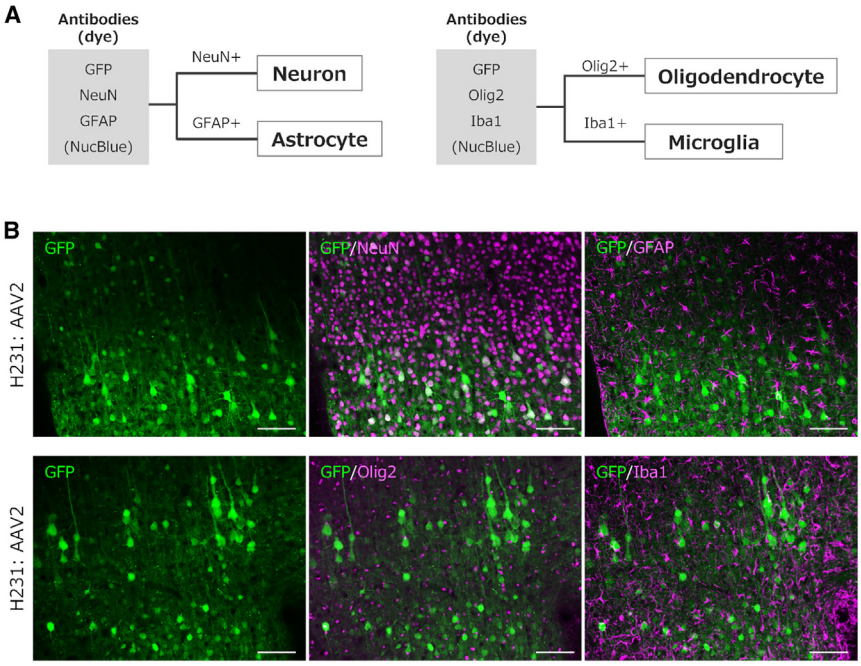

Figure 2. Identification of cell types by fluorescent immunohistochemistry (fIHC)

(A) Schematic representation of EGFP-expressing cell types obtained by IHC. Neurons and astrocytes were immunolabeled for NeuN and GFAP, respectively. Cells immunostained for Olig2 and Iba1 were identified as oligodendrocytes and microglia, respectively. The cells were detected using Hoechst 33342 (NucBlue) with the mounting reagent ProLong Glass. (B) Representative IHC images of the marmoset cerebral cortex that received the AAV2 injection. Two serial slices are presented: one immunolabeled for GFP, NeuN, and GFAP and the other for GFP, Olig2, and Iba1, as indicated in each panel. Scale bar, 100 μm.

the animals were sacrificed for fIHC. Fluorescent microscopy revealed numerous astrocyte-like EGFP-expressing cells in all the cortices injected with the nine serotypes (Figure 5B). Subsequent fIHC analysis confirmed that most of the EGFP-labeled cells in the cortical sections injected with any of the nine serotypes were immunolabeled for GFAP, confirming efficient astrocyte transduction by capsids of all nine serotypes (Figures 5C and 5D). Although the difference was not statistically significant, AAV2 and AAV7 consistently expressed EGFP in astrocytes with higher specificity than the other tested serotypes (Figure 5D).

AAV5 and AAV8 induced transgene expression in astrocytes with lower specificity (Figure 5D). We examined the results for individual marmosets and found that one marmoset (ID: H271, see Table 1) showed markedly low specificity for cortical astrocytes when injected with AAV5 or AAV8. To identify cell types other than astrocytes expressing EGFP, the cortical sections were immunostained with anti-Olig2 and anti-Iba1 antibodies. The results revealed that all EGFP-expressing non-astrocytes were immunolabeled for Olig2 (Figure S5), indicating that they were oligodendrocytes.

Since AAV5 carrying the CBh promoter also showed consistently higher specificity for oligodendrocytes than many other serotypes (Figure 3C), we hypothesized that the AAV5 capsid may have tropism for oligodendrocytes. If the AAV5 capsid is oligodendrocyte-tropic, then AAV5 with an oligodendrocyte-specific promoter could achieve efficient and specific transgene expression in marmoset oligodendrocytes. To validate this hypothesis, we produced an AAV5 capsid vector expressing EGFP using an oligodendrocyte-specific mouse-derived myelin basic protein (mMBP) promoter (Figure 6A). The AAVrh10 capsid was used as a control because this capsid-coated CBh promoter-driven AAV is highly neurotropic and expresses EGFP in oligodendrocytes less effectively than AAV5 (Figures 3B and 3C).

Four weeks after the viral injection, the animals were sacrificed for fIHC. Immunostaining of the cortical sections showed numerous EGFP-expressing cells co-immunolabeled with Olig2 in the marmosets injected with AAV5 (Figure 6B), in contrast to the much lower frequency of simultaneous immunolabeling with EGFP and Olig2 in the marmosets injected with AAVrh10 (Figure 6C). Quantitative results showed that over 80% of EGFP-expressing cells were Olig2$^+$ oligodendrocytes in marmosets injected with AAV5 (81.8% ± 5.7%, n = 4 marmosets), which were significantly higher than marmosets injected with AAVrh10 (30.6% ± 5.0%, n = 4 marmosets, $^*p$ = 0.029 by permuted Brunner-Munzel test) (Figure 6D). In addition, the efficiency of transgene expression in oligodendrocytes was significantly higher in marmosets injected with AAV5 (68.8% ± 1.1%, n = 4 marmosets) than in marmosets injected with AAVrh10 (39.2% ± 5.7%, n = 4 marmosets, $^*p$ = 0.029 by permuted Brunner-Munzel test) (Figure 6E). If the mMBP promoter is highly specific to oligodendrocytes, regardless of the capsid used, then transgene expression should be observed primarily in oligodendrocytes. Therefore, the specificity of the mMBP promoter may not be high in marmoset oligodendrocytes. Furthermore, our results suggest that in cases where the specificity of the promoter for the target cell type is not sufficiently high, the specificity to the target cell type and expression efficiency are greatly influenced by the cellular affinity of the capsid.

DISCUSSION

In the present study, we injected nine AAV serotypes expressing EGFP into the marmoset cerebral cortex and investigated the tropism of different cortical cell types in the marmoset brain. Although not statistically significant, AAV1, AAV9, AAVrh10, and AAV-DJ induced widespread EGFP expression. Subsequent IHC showed that all serotypes with the CBh promoter expressed EGFP primarily in neurons. Considering the spread of the EGFP expression region, AAV9, AAVrh10, and AAV-DJ are suitable for the efficient expression of transgenes in marmoset cortical neurons.

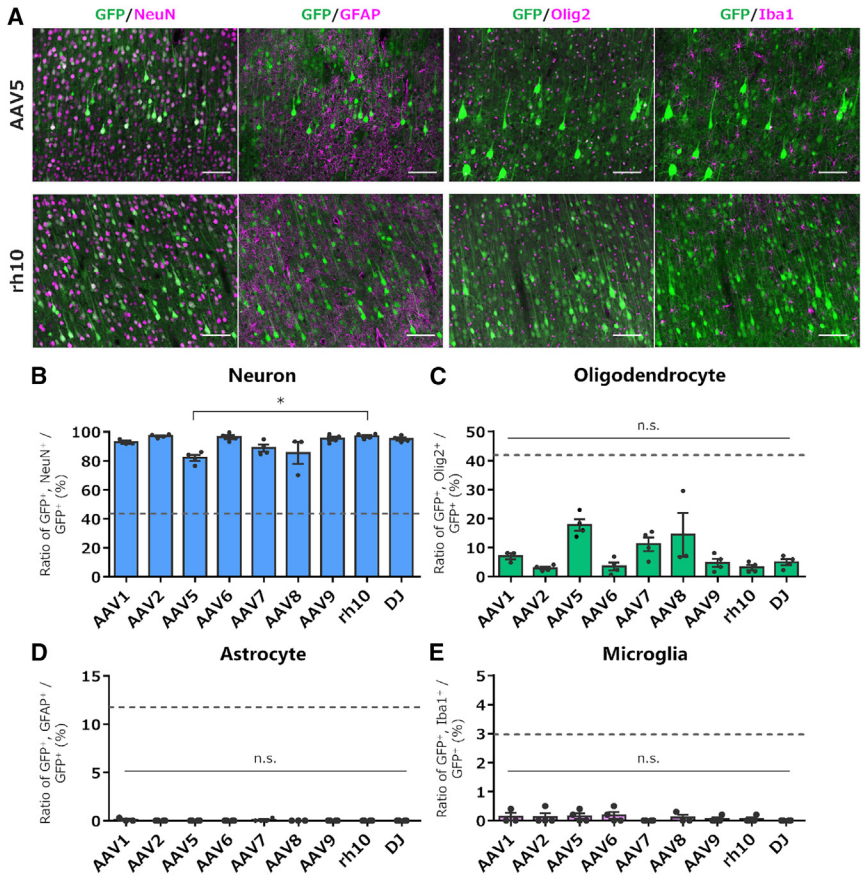

Figure 3. Quantitative analysis of EGFP-expressing cell types following injection of nine serotype AAV vectors into the marmoset cerebral cortex

(A) Representative fluorescent images of the cortical sections immunostained for GFP (green), NeuN, GFAP, Olig2, and Iba1 (magenta) 4 weeks after injection of AAV5 or AAVrh10. Scale bar, 100 μm. (B–E) Graphs showing the ratio of GFP^+ neurons (B), GFP^+ oligodendrocytes (C), GFP^+ astrocytes (D), and GFP^+ microglia (E) to total GFP^+ cells. The dotted lines in the graphs are ratios of respective cell types to total cells present in the marmoset cortex (see Figure S3). Error bars indicate SEM, and the dots in the graph indicate the respective values for each of the individual marmosets. The asterisks indicate a statistically significant difference between the AAV5 vector and AAVrh10. *$p < 0.05$ by a Kruskal-Wallis test with Dunn's post hoc test. n.s., not significant.

Watakabe et al. studied the tropism of five AAV serotype capsids (AAV1, 2, 5, 8, and 9) with the CMV promoter, neuron-specific mouse calcium-calmodulin-dependent protein kinase II, or human synapsin I promoter in marmoset cerebral cortical cell types.[11] In contrast to our results, the injection of AAV1, 5, 8, and 9 carrying the CMV promoter led to glial cell-dominant transgene expression. The differences between the experiments of Watakabe et al. and ours are that they used an approximately 4-fold higher dose of AAV vectors than we used here and that they used hrGFP as a transgene. It has been reported that hrGFP is more toxic to muscle cells than EGFP when expressed in large amounts.[22] Consequently, they observed tissue damage, such as decreased expression levels of NeuN, neuron loss, and glial infiltration, in cortical tissue injected with AAV vectors expressing hrGFP under the control of the CMV promoter. Interestingly, such findings were not observed when a neuron-specific promoter was used, probably because of the weaker promoter strength and lower expression levels of hrGFP compared with the CMV promoter. Thus, tissue damage was likely caused by the combination of high injection doses of AAV vectors and the overexpression of hrGFP by the CMV promoter.

In the present study, using AAV2 expressing EGFP under the control of the CBh promoter, we determined the appropriate injection dose that did not cause local inflammation (6.0×10^8 vg). Although the optimal viral titer for other serotypes may differ from that for AAV2, we did not observe decreased NeuN expression, cell loss, or morphological changes in microglia in areas injected with serotypes other than AAV2 (Figures 3A and S4), suggesting that other serotypes did not cause obvious tissue damage or inflammation at this dose.

The CBh, CMV, and CAG promoters are constitutive promoters active in a variety of cell types.[23–25] However, regardless of serotype, AAV-mediated transgene expression driven by these promoters was largely detected in neurons, with sparse expression in glial cells in the cerebral cortex of marmosets. Notably, no astrocytes expressed EGFP in the CBh or CMV promoters (Figures 3D and 4D). Similar results have been reported previously, which showed high neurotropic transgene expression following direct injection of AAV8 or AAV9 with the CAG promoter in the marmoset brain.[12,13] Thus, the constitutive CBh, CMV, and CAG promoters, which were delivered by parenchymal injection of AAV, worked specifically on neurons in the marmoset brain.

The finding of little or no EGFP expression in glial cells of the marmoset cortex by AAV vectors with ubiquitously active CBh, CMV, or CAG promoters does not indicate that the AAV serotypes tested do not have the ability to infect glial cells, because all nine serotypes efficiently expressed EGFP in astrocytes when the astrocyte-specific hGFA(ABC1D) promoter was used, and AAV5 and AAVrh10 with the oligodendrocyte-specific mMBP promoter expressed EGFP in oligodendrocytes (Figures 5 and 6). Therefore, all nine AAV serotype capsids appear to be tropic, not only to neurons but also to astrocytes and oligodendrocytes. However, for microglia in the marmoset cortex, it remains unclear whether the AAV serotypes used are unable to infect microglia or whether the promoter used is activated in microglia.

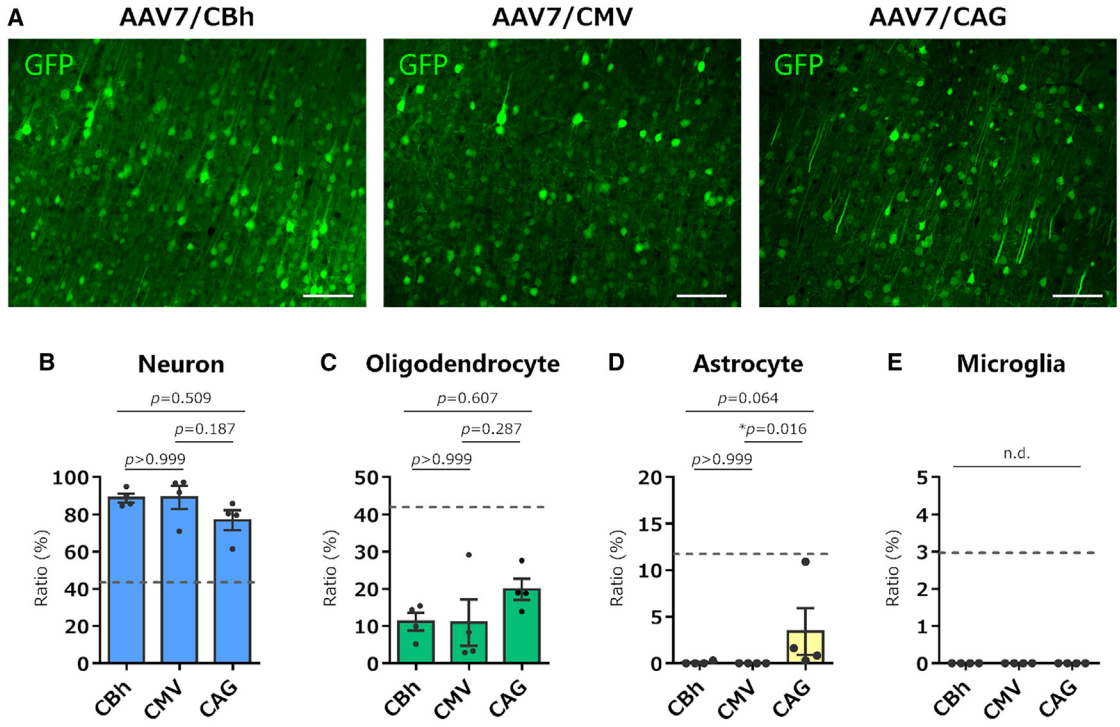

Figure 4. No or little EGFP expression in marmoset cortical glial cells by AAV vectors expressing EGFP under the control of three different ubiquitous promoters

(A) Immunofluorescent EGFP images of the cortex injected with AAV7 expressing EGFP by the CBh, CMV, or CAG promoter. Scale bar, 100 μm. (B–E) Graphs showing ratios of respective EGFP-immunolabeled cell types to total EGFP-expressing cells by AAV7 vectors with the CBh, CMV, and CAG promoters. The dotted lines in the graphs are ratios of respective cell types to total cells present in the marmoset cortex (see Figure S3). Error bars indicate SEM, and dots in the graph indicate the respective values for each of the individual marmosets. *$p < 0.05$ by a Kruskal-Wallis test with Dunn's post hoc test was described in the graphs. n.d., not detected.

In our previous studies, intravenous injection of AAV9 capsid variants that penetrate the blood-brain barrier (BBB) has often been used to express transgenes in the mouse brain.[24,26–28] Several AAV9-derived capsid variants that penetrate the marmoset BBB have been reported[29–31]; they are not as effective as mouse BBB-crossing capsid mutants, such as PHP.eB[23] and AAV-F.[32] Furthermore, serotype capsids other than AAV9 only have a modest ability to cross the BBB. Therefore, in the present study, we injected AAV vectors directly into the brain parenchyma of marmosets. This method allows injections at approximately 10 locations in the cerebral cortex of one marmoset, making it possible to significantly reduce the number of marmosets used. However, although we decided on the optimal AAV dose that did not cause obvious inflammation, brain parenchymal injections inevitably caused tissue damage due to needle insertion, which could activate glial cells and influence the cell-type tropism of AAV capsids. Indeed, when AAV9 was administered intravenously, the CBh promoter triggered EGFP expression in astrocytes of the marmoset cerebral cortex,[33] but when AAV9 was administered directly to the brain parenchyma, the same CBh promoter did not work in astrocytes (Figure 3D). Thus, CBh, CMV, and CAG promoter activities may be suppressed in reactive astrocytes.

Despite the use of an oligodendrocyte-specific mMBP promoter, the specificity and efficiency of transgene expression in oligodendrocytes differed significantly between AAV5 and AAVrh10 (Figure 6). AAV5 caused EGFP expression in oligodendrocytes with a high specificity of over 80%, whereas the specificity of EGFP expression in oligodendrocytes by AAVrh10 was as low as 31%, which was less than the proportion of oligodendrocytes (approximately 42%) in the total cortical cells (Figures 6E and S3). Our results suggested that AAV5 is suitable for targeting marmoset oligodendrocytes. The oligodendrocyte specificity (approximately 80%) of AAV5 carrying the mMBP promoter may be improved by switching the MBP promoter from that derived from the mouse to that derived from the marmoset genome, as observed for the GFAP promoter.[34]

Although significant differences in specificity between serotypes, as seen in oligodendrocytes, were not observed in astrocytes, AAV2 and AAV7 stably expressed EGFP in astrocytes with higher specificity than the other serotypes; thus, AAV2 and AAV7 are thought to be suitable for targeting marmoset astrocytes. Similar to the oligodendrocyte-specific mMBP promoter in combination with the neuron-tropic AAVrh10 capsid that led to the expression of EGFP in non-oligodendrocytes, the astrocyte-specific

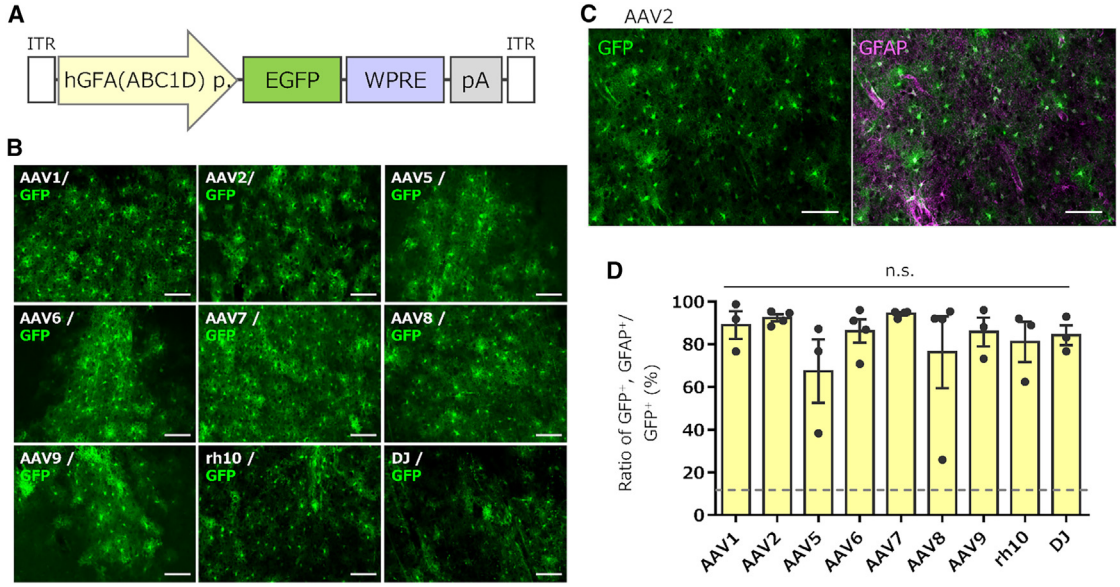

Figure 5. Efficient EGFP expression in astrocytes by all nine serotype AAVs with the astrocyte-specific hGFA(ABC1D) promoter

(A) Schema depicting the AAV genome structure. (B) Immunofluorescent EGFP images of the cerebral cortex received injections of respective AAV vectors. Scale bar, 100 μm. (C) Representative image immunostained for EGFP alone (left) and merged image for EGFP and GFAP (right) after injection of the AAV2 vector. Scale bar, 100 μm. (D) Graph showing the percentage of $GFAP^+$ astrocytes to total EGFP-expressing cells 4 weeks after injection of the AAV vector as indicated. The dotted line in the graph shows a ratio of astrocytes to total cells present in the marmoset cortex (see Figure S3). Error bars indicate SEM, and dots in the graph indicate the respective values for each of the individual marmosets. n.s., not statistically significant by a Kruskal-Wallis test with Dunn's post hoc test.

hGFA(ABC1D) promoter in combination with oligodendrocyte-tropic AAV5 led to the expression in a large number of oligodendrocytes (Figure S5). These results suggest that although the mMBP and hGFA(ABC1D) promoters function as their respective target cell-type-specific promoters in marmosets, cell type specificity is greatly compromised when using a capsid with low affinity for the target cell type.

Using marmosets, we showed that nine AAV serotypes can infect neurons, astrocytes, and oligodendrocytes with distinct tropisms. It seems likely that the activities of the CBh, CMV, and CAG promoters are significantly suppressed in glial cells and that they function as neuron-specific promoters when AAV vectors are injected directly into the marmoset cerebral cortex. Our results suggest that AAV2 and AAV7 with hGFA(ABC1D) promoters are suitable for transgene expression in astrocytes, whereas AAV5 with the mMBP promoter is suitable for transgene expression in oligodendrocytes. Therefore, selecting an appropriate promoter and capsid is important to efficiently and specifically achieve target cell-specific transgene expression in the marmoset brain.

MATERIALS AND METHODS

Animals

The present study included 19 common marmosets (*Callithrix jacchus*) (summarized in Table 1). All the marmosets were bred at the Gunma University Bioresource Center. The animals were maintained in breeding rooms under controlled temperature (27°C–30°C), humidity (25%–45%), and light cycle (12 h each of light and dark) conditions. The marmosets were allowed to drink filtered water *ad libitum*. We fed 45–50 g of soaked monkey chow (CMS-1; CLEA Japan, Tokyo, Japan) with fruits, vegetables, or boiled chicken around 12 p.m., and marmoset dumplings made by mixing CMS-1 soaked in hot water, honey, oligosaccharide, milk powder, vitamin supplement, Lactobacillus powder, and gum arabic powder around 3 p.m. on a weekday afternoon. Cages and living spaces were suitable for the *Guide for the Care and Use of Laboratory Animals*, 8th edition. All efforts were made to minimize suffering and reduce the number of animals used, and all procedures regarding animal care and treatment were performed in accordance with guidelines approved by the Japan Neuroscience Society (*Guidelines for the Care and Use of Nonhuman Primates in Neuroscience Research*) and the Institutional Committee of Gunma University (approval nos. 20–053, 21–063, and 23–057).

Construction of plasmids

The expression plasmids pAAV-CBh-EGFP-WPRE-HBGpA, pAAV-CMV-EGFP-WPRE-HBGpA, and pAAV-CAG-EGFP-WPRE-SV40pA were used as expression plasmids for constitutive expression of EGFP by the CBh, CMV, and CAG promoters, respectively.[14,20,35] These promoters were inserted into the expression plasmid pAAV immediately upstream of EGFP at the restriction enzyme sites for XhoI and AgeI. The astrocyte-specific hGFA(ABC1D) promoter from the pZac2.1-gfaABC1D-cyto-GCaMP6f gifted by Baljit Khakh (Addgene plasmid no. 52925; http://n2t.net/addgene:52925; RRID: Addgene_52925) was amplified by KOD One PCR Master Mix (KMM-201; Toyobo, Osaka,

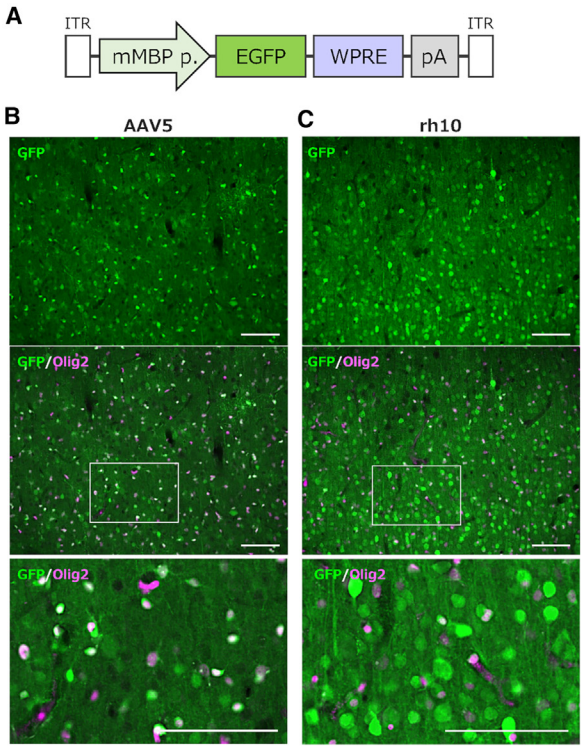

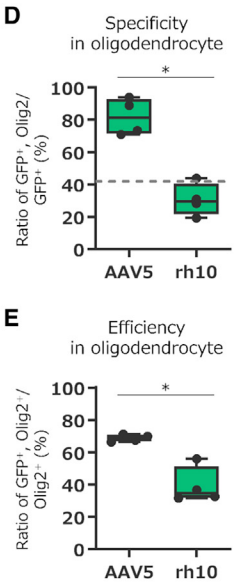

Figure 6. Selective and efficient transgene expression in marmoset oligodendrocytes by AAV5 vectors with mouse myelin basic protein (mMBP) promoter

(A) Schema depicting the AAV genome structure. (B and C) Immunolabeled fluorescent images of EGFP in the cerebral cortex that received injection of AAV5 (B) or AAVrh10 (C) vectors expressing EGFP by the mMBP promoter. The center immunofluorescence images present an overlay of immunolabeling for EGFP and the oligodendrocyte marker Olig2. The bottom images are magnifications of the boxed areas in the center images. Scale bar, 100 μm. (D and E) Summary graphs showing the specificity (D) and efficiency (E) of transgene expression in oligodendrocytes. The dotted line in the graph indicates a ratio of oligodendrocytes to total cells present in the marmoset cortex (see Figure S3). Box and whisker plots display the median (centerline), 25th–75th percentile (box), and minimum–maximum values (whiskers); black dots indicate data for each marmoset. Asterisks indicate statistically significant differences between the AAV5 and AAVrh10. *$p < 0.05$ by permuted Brunner-Munzel test.

Japan) using the following primers: 5′-ATGCTCTAGACTCGAGAACATATCCTGGTG-3′ and 5′-CATGGTGGCGACCGGTGCGAGCAGC-3′ to create the pAAV-hGFAP(ABC1D)-EGFP-WPRE-SV40pA.[36] The oligodendrocyte-specific mMBP promoter was amplified from the pAAV-MBP-2xNLS-tdTomato gift from Viviana Gradinaru (Addgene plasmid no. 104054; http://n2t.net/addgene:104054; RRID: Addgene_104054) by KOD One PCR Master Mix using following primers 5′-ATGCTCTAGACTCGAGTCCTTCCTGCTTAGGCCGTG-3′ and 5′-CATGGTGGCGACCGGTCCTCCGGAAGCTGCTGTGGG-3′ to create the pAAV-mMBP-EGFP-WPRE-SV40pA.[37] The PCR-amplified promoter fragments were inserted into the XhoI-AgeI site of the pAAV using Ligation high version 2 (LGK-201; Toyobo: hGFAP(ABC1D) or In-Fusion HD Cloning Kit (TaKaRa Bio, Shiga, Japan: mMBP promoter).

The rep/cap plasmids pRC1 (TaKaRa Bio), pAAV2/5 (gift from Melina Fan [Addgene plasmid no. 104964; http://n2t.net/addgene:104964; RRID: Addgene_104964]), pAAV2/7 (gift from James M. Wilson [Addgene plasmid no. 112863; http://n2t.net/addgene:112863; RRID: Addgene_112863]), pAAV2/8 (gift from James M. Wilson [Addgene plasmid no. 112864; http://n2t.net/addgene:112864; RRID: Addgene_112864]) and pAAV2/AAVrh10 (gift from James M. Wilson [Addgene plasmid no. 112866; http://n2t.net/addgene:112866; RRID: Addgene_112866]) were obtained from Addgene. pAAV-DJ was purchased from Cosmo Bio (VPK-420-DJ; Cell Biolabs, San Diego, CA). pRC2-mi342, which was used to produce the AAV2/2 vector, was included in the AAVpro Helper Free System (TaKaRa Bio). The AAV2/9 plasmid was provided by James M. Wilson. To construct the rep/cap plasmid pAAV2/6, we replaced the cap8 gene in pAAV2/8 (Addgene plasmid no. 112864) with the cap6 gene in pRepCap6 (a gift from David Russell [Addgene plasmid no. 110770; http://n2t.net/addgene:110770; RRID: Addgene_110770]). Gene engineering experiments were approved by the institutional committee of Gunma University (approval nos. 20-018 and 23–056).

Production of AAV vectors

Eight AAV serotypes, except for AAV2, were collected from the culture supernatant. Recombinant single-stranded AAV vectors were produced using the ultracentrifugation method described in a previous study using HEK293T cells (HCL4517; Thermo Fisher Scientific, Waltham, MA), as described by Konno and Hirai.[38] Briefly, HEK293T cells, which were cultured in DMEM (D5796-500ML, Merck, Darmstadt, Germany) supplemented with 8% fetal bovine serum (26140-079, Sigma-Aldrich) at 37°C in 5% CO_2, were transfected with three plasmids: an expression plasmid pAAV, pHelper (Stratagene, La Jolla, CA), and a rep/capsid plasmid using polyethylenimine "Max" (24765-1; Polysciences, Warrington, PA). Viral particles were harvested from the culture medium 6 days after transfection and concentrated by precipitation with 8% polyethylene glycol 8000 (Merck) and 500 mM sodium chloride. The precipitated AAV vectors were resuspended in DPBS(-) and purified using iodixanol (OptiPrep; Serumwerk Bernburg AG, Bernburg, Germany) by continuous gradient centrifugation. The viral solution was further concentrated in DPBS(-) using a Vivaspin turbo 15 (100,000 molecular weight cutoff polyethersulfone; Sartorius, Gottingen, Germany).

In addition, Dr. Hioki of the Brain/MINDS Viral Vector Core provided us with AAV2/CBh-EGFP and AAV2/hGFA(ABC1D)-EGFP vectors extracted from inside and outside cells. AAV vector particles were produced and purified as previously described.[39,40] Briefly, pAAV-CBh-EGFP-WPRE-HBGpA or pAAV-hGFA(ABC1D)-EGFP-WPRE-SV40pA and two helper plasmids, pBSIISK-R2C1 and pHelper (Merck; GenBank: AF369965.1), were co-transfected into HEK293T cells (RCB2202; Riken BRC) using polyethylenimine (23966, Polysciences). Viral particles were purified from the cell lysate and supernatant by ultracentrifugation with OptiPrep (Serumwerk Bernburg AG) and concentrated by ultrafiltration with Amicon Ultra-15 (UFC903024, Merck).

The genomic titers of the viral vectors were determined by real-time qPCR using Thermal Cycler Dice Real Time System II TP900 or III TP970 (TaKaRa Bio) and Power SYBR Green PCR Master Mix (Thermo Fisher Scientific) using the primers 5′-CTGTTGGGCACTGACAATTC-3′ and 5′-GAAGGGACGTAGCAGAAGGA-3′, which targeted the WPRE sequence. The expression plasmid was used as a standard to plot absolute quantitation. The produced AAVs were stored at 4°C for a few months or less and at −80°C for longer storage. AAV2 vectors were frozen and stored at −80°C.

Cerebral cortical parenchymal viral administration

To immobilize the marmosets during parenchymal administration, the marmosets were anesthetized with a cocktail of ketamine hydrochloride (20–25 mg/kg) and xylazine hydrochloride (4–5 mg/kg) and maintained in the anesthetic state with isoflurane (2%–2.5% in 60%–70% O_2, 1 L/min) using an anesthesia apparatus (NARCOBIT-E(II), KN-1071; Natsume Seisakusho, Tokyo, Japan). The SpO_2 concentration and heart rate were monitored using a pulse oximeter (OLV-2700; Nihon Kohden, Tokyo, Japan). The marmoset was held in a brain stereotaxic instrument (SR-5C-HT; Narishige, Tokyo, Japan), and a thermal seat was used to maintain its body temperature. After making a scalpel incision, a hole was drilled into the skull against the viral administration point using an electric drill (DC Power Pack C2012 and handpiece Minimo SD-101 attaching carbide cutter BC1403 or steel drill KA1001; Minitor, Tokyo, Japan). A 30G or 32G needle with a 1- to 2-mm angled tip was used to confirm that the skull had been punctured and to simultaneously injure the meninges. The AAV solutions were loaded into a 33G Hamilton syringe (701SN 33G 2”/PT3, 80308; Hamilton, Reno, NV) and set into a microinjector (IMS-30; Narishige) attached to a stereotaxic instrument. The needle was inserted 1 mm below the base of the skull, and AAV solutions were administered at a flow rate of 0.1 μL/min. After all viral injections were completed, the holes were plugged with medical-grade Aron Alpha A (Daiichi Sankyo, Tokyo, Japan) and sutured using a synthetic absorbable suture. Finally, to prevent the marmosets from scratching the sutures and making incisions with their fingernails, a liquid adhesive plaster, Coloskin (Tokyo Koshi, Tokyo, Japan), was used to cover the sutures and wounds. Ampicillin (5 mg) was administered for 5 days to prevent infection.

Necropsy

Sacrifice was performed 4 weeks after AAV injection. The marmosets were anesthetized with a cocktail of ketamine hydrochloride, xylazine hydrochloride, and isoflurane. Marmosets were perfused with 300 mL of cold 1× PBS(-) containing 20 mM EDTA (311-90075, Nippon Gene, Tokyo, Japan), fixed with 250 mL of cold 4% paraformaldehyde (PFA) in 1× phosphate buffer, and the brains were removed. GFP fluorescence on the brain surface was captured by fluorescence microscopy (VB-7010; Keyence, Osaka, Japan), and the brains were post-fixed in 4% PFA overnight.

fIHC analysis

Brain slices were prepared for the GFP expression analysis. Marmoset brains were trimmed except for the cerebrum and embedded in 2% agarose gel to make 100-μm-thick sagittal sections using a microtome (VT1200S; Leica Microsystems GmbH, Wetzlar, Germany). Sections were stored at 4°C in 1× PBS(-) with NaN_3 until use. fIHC was performed on free-floating cells to identify GFP expression in tissues and various types of brain cells. Tissues were stained quadruple-fluorescently, including nuclear staining with NucBlue (Hoechst 33342). Tissue sections were reacted overnight at room temperature by immersion in the following primary antibodies in blocking solution (2% Donkey Serum [S30-100ML, Merck], BSA [A9647, Merck], 0.5% Triton X-100, 0.03% NaN_3 in 1× phosphate buffer): rat monoclonal anti-GFP antibody (1:1,000; 04404-84; Nacalai Tesque, Kyoto, Japan), mouse monoclonal anti-NeuN antibody (1:1,000; MAB377; Merck), rabbit polyclonal anti-GFAP antibody (1:200; GFAP-Rb-Af800; Nittobo Medical, Tokyo, Japan), rabbit polyclonal anti-S100β antibody (1:200; S100b-Rb-Af1000, Nittobo Medical), mouse monoclonal anti-Olig2 antibody (1:500; MABN50; Merck), and rabbit polyclonal anti-Iba1 antibody (1:500; 019-19741; Fujifilm Wako Chemicals, Tokyo, Japan). To visualize the bound primary antibodies, the sections were incubated for 3–4 h at room temperature in a blocking solution containing the following secondary antibodies: donkey anti-rat immunoglobulin G (IgG) Alexa Fluor Plus 488, donkey anti-mouse IgG Alexa Fluor Plus 555, donkey anti-rabbit IgG Alexa Fluor Plus 555, and donkey anti-rat IgG Alexa Fluor Plus 647 (1:2,000, Thermo Fisher Scientific). After the secondary antibody reaction, they were sealed in glass slides using ProLong Glass Antifade Mountant with NucBlue Stain (Thermo Fisher Scientific), cured, and stored at 4°C.

The immunostained slices were photographed under a fluorescence microscope (BZ-X800; Keyence). Images used for cell counting were captured at each injection site using the same exposure time settings and sectioning functions. All images for cell-type counting were obtained using a 20× objective and had an area of 0.394 mm^2. A consolidated image of 0.672 mm^2 was used for counting the number of cells of each endogenous cell type. Cells were counted on the images using the free software Katikati Counter (https://www.vector.co.jp/soft/win95/art/se347447.html).

Statistical analysis

GraphPad Prism versions 6 and 10 (GraphPad Software, San Diego, CA) and R (R Foundation for Statistical Computing, Vienna, Austria;

https://www.R-project.org/) were used for statistical analysis and output of graphic images. ANOVA among multiple groups was performed using the Kruskal-Wallis test with Dunn's multiple comparison test. A permuted Brunner-Munzel test was used to compare the results of the two groups. An open-source package for R was used for this test (Ara T, 2022, brunnermunzel: (Permuted) Brunner-Munzel Test, R package version 2.0). Each set of data with multiple groups is expressed as scatterplots with bar graphs. Bars indicate mean values, error bars indicate SEM, and black dots indicate data for each marmoset. The dataset with two groups is expressed as box and whisker plots that displayed the median (centerline), 25th–75th percentile (box), and minimum–maximum values (whiskers), and black dots indicate data for each marmoset.

DATA AND CODE AVAILABILITY

The datasets and programs generated in this study are available from the corresponding author upon request.

ACKNOWLEDGMENTS

The authors thank Asako Ohnishi, Nobue McCullough, and Chieko Miyazawa for AAV1, 5, 6, 7, 8, 9, rh10, and DJ vector production; Prof. Hiroyuki Hioki and Project Assistant Prof. Megumu Takahashi at Juntendo University for AAV2 vector production; Motoko Uchiyama, Minako Noguchi, and Yoshiko Nomura for raising the marmosets; Junko Sugi for IHC; and Associate Prof. Yuki Ideno at Gunma University, Center for Mathematics and Data Science, for consultation on the statistical analysis. This research was partially supported by the Program for Brain Mapping by Integrated Neurotechnologies for Disease Studies (Brain/MINDS) of the Japan Agency for Medical Research and Development (AMED) (JP20dm0207057, JP21dm0207111, and JP21dm0207112), JSPS KAKENHI (grant nos. 24K15743, 24H01221, 23H02791, and 22K06454), and Gunma University for the promotion of scientific research.

AUTHOR CONTRIBUTIONS

H.H. supervised this study. Y.M., A.K., and H.H. designed the experiments. Y.M., Y.F., and A.K. performed the experiments. Y.M. prepared the original draft. All the authors have read and approved the final version of the manuscript.

DECLARATION OF INTERESTS

The authors declare no competing interests.

SUPPLEMENTAL INFORMATION

Supplemental information can be found online at https://doi.org/10.1016/j.omtm.2024.101337.

REFERENCES

1. Jäkel, S., Agirre, E., Mendanha Falcão, A., van Bruggen, D., Lee, K.W., Knuesel, I., Malhotra, D., Ffrench-Constant, C., Williams, A., and Castelo-Branco, G. (2019). Altered human oligodendrocyte heterogeneity in multiple sclerosis. Nature *566*, 543–547. https://doi.org/10.1038/s41586-019-0903-2.

2. López-Muguruza, E., and Matute, C. (2023). Alterations of Oligodendrocyte and Myelin Energy Metabolism in Multiple Sclerosis. Int. J. Mol. Sci. *24*, 12912. https://doi.org/10.3390/ijms241612912.

3. Busche, M.A., and Hyman, B.T. (2020). Synergy between amyloid-β and tau in Alzheimer's disease. Nat. Neurosci. *23*, 1183–1193. https://doi.org/10.1038/s41593-020-0687-6.

4. Haney, M.S., Pálovics, R., Munson, C.N., Long, C., Johansson, P.K., Yip, O., Dong, W., Rawat, E., West, E., Schlachetzki, J.C.M., et al. (2024). APOE4/4 is linked to damaging lipid droplets in Alzheimer's disease microglia. Nature *628*, 154–161. https://doi.org/10.1038/s41586-024-07185-7.

5. Shi, K., Tian, D.C., Li, Z.G., Ducruet, A.F., Lawton, M.T., and Shi, F.D. (2019). Global brain inflammation in stroke. Lancet Neurol. *18*, 1058–1066. https://doi.org/10.1016/s1474-4422(19)30078-x.

6. Xu, S., Lu, J., Shao, A., Zhang, J.H., and Zhang, J. (2020). Glial Cells: Role of the Immune Response in Ischemic Stroke. Front. Immunol. *11*, 294. https://doi.org/10.3389/fimmu.2020.00294.

7. Aschauer, D.F., Kreuz, S., and Rumpel, S. (2013). Analysis of transduction efficiency, tropism and axonal transport of AAV serotypes 1, 2, 5, 6, 8 and 9 in the mouse brain. PLoS One *8*, e76310. https://doi.org/10.1371/journal.pone.0076310.

8. Cearley, C.N., Vandenberghe, L.H., Parente, M.K., Carnish, E.R., Wilson, J.M., and Wolfe, J.H. (2008). Expanded repertoire of AAV vector serotypes mediate unique patterns of transduction in mouse brain. Mol. Ther. *16*, 1710–1718. https://doi.org/10.1038/mt.2008.166.

9. Cearley, C.N., and Wolfe, J.H. (2006). Transduction characteristics of adeno-associated virus vectors expressing cap serotypes 7, 8, 9, and Rh10 in the mouse brain. Mol. Ther. *13*, 528–537. https://doi.org/10.1016/j.ymthe.2005.11.015.

10. Hutson, T.H., Verhaagen, J., Yáñez-Muñoz, R.J., and Moon, L.D.F. (2012). Corticospinal tract transduction: a comparison of seven adeno-associated viral vector serotypes and a non-integrating lentiviral vector. Gene Ther. *19*, 49–60. https://doi.org/10.1038/gt.2011.71.

11. Watakabe, A., Ohtsuka, M., Kinoshita, M., Takaji, M., Isa, K., Mizukami, H., Ozawa, K., Isa, T., and Yamamori, T. (2015). Comparative analyses of adeno-associated viral vector serotypes 1, 2, 5, 8 and 9 in marmoset, mouse and macaque cerebral cortex. Neurosci. Res. *93*, 144–157. https://doi.org/10.1016/j.neures.2014.09.002.

12. Masamizu, Y., Okada, T., Ishibashi, H., Takeda, S., Yuasa, S., and Nakahara, K. (2010). Efficient gene transfer into neurons in monkey brain by adeno-associated virus 8. Neuroreport *21*, 447–451. https://doi.org/10.1097/WNR.0b013e328338ba00.

13. Masamizu, Y., Okada, T., Kawasaki, K., Ishibashi, H., Yuasa, S., Takeda, S., Hasegawa, I., and Nakahara, K. (2011). Local and retrograde gene transfer into primate neuronal pathways via adeno-associated virus serotype 8 and 9. Neuroscience *193*, 249–258. https://doi.org/10.1016/j.neuroscience.2011.06.080.

14. Gray, S.J., Foti, S.B., Schwartz, J.W., Bachaboina, L., Taylor-Blake, B., Coleman, J., Ehlers, M.D., Zylka, M.J., McCown, T.J., and Samulski, R.J. (2011). Optimizing promoters for recombinant adeno-associated virus-mediated gene expression in the peripheral and central nervous system using self-complementary vectors. Hum. Gene Ther. *22*, 1143–1153. https://doi.org/10.1089/hum.2010.245.

15. Li, C., and Samulski, R.J. (2020). Engineering adeno-associated virus vectors for gene therapy. Nat. Rev. Genet. *21*, 255–272. https://doi.org/10.1038/s41576-019-0205-4.

16. Donato, R. (2001). S100: a multigenic family of calcium-modulated proteins of the EF-hand type with intracellular and extracellular functional roles. Int. J. Biochem. Cell Biol. *33*, 637–668. https://doi.org/10.1016/s1357-2725(01)00046-2.

17. Eng, L.F., and Ghirnikar, R.S. (1994). GFAP and astrogliosis. Brain Pathol. *4*, 229–237. https://doi.org/10.1111/j.1750-3639.1994.tb00838.x.

18. Ransom, B., Behar, T., and Nedergaard, M. (2003). New roles for astrocytes (stars at last). Trends Neurosci. *26*, 520–522. https://doi.org/10.1016/j.tins.2003.08.006.

19. Miyazaki, J., Takaki, S., Araki, K., Tashiro, F., Tominaga, A., Takatsu, K., and Yamamura, K. (1989). Expression vector system based on the chicken beta-actin promoter directs efficient production of interleukin-5. Gene *79*, 269–277. https://doi.org/10.1016/0378-1119(89)90209-6.

20. Niwa, H., Yamamura, K., and Miyazaki, J. (1991). Efficient selection for high-expression transfectants with a novel eukaryotic vector. Gene *108*, 193–199. https://doi.org/10.1016/0378-1119(91)90434-d.

21. Lee, Y., Messing, A., Su, M., and Brenner, M. (2008). GFAP promoter elements required for region-specific and astrocyte-specific expression. Glia *56*, 481–493. https://doi.org/10.1002/glia.20622.

22. Wallace, L.M., Moreo, A., Clark, K.R., and Harper, S.Q. (2013). Dose-dependent Toxicity of Humanized Renilla reniformis GFP (hrGFP) Limits Its Utility as a Reporter Gene in Mouse Muscle. Mol. Ther. Nucleic Acids *2*, e86. https://doi.org/10.1038/mtna.2013.16.

23. Chan, K.Y., Jang, M.J., Yoo, B.B., Greenbaum, A., Ravi, N., Wu, W.L., Sánchez-Guardado, L., Lois, C., Mazmanian, S.K., Deverman, B.E., and Gradinaru, V. (2017). Engineered AAVs for efficient noninvasive gene delivery to the central and

peripheral nervous systems. Nat. Neurosci. *20*, 1172–1179. https://doi.org/10.1038/nn.4593.

24. Kawabata, H., Konno, A., Matsuzaki, Y., Sato, Y., Kawachi, M., Aoki, R., Tsutsumi, S., Togai, S., Kobayashi, R., Horii, T., et al. (2024). Improving cell-specific recombination using AAV vectors in the murine CNS by capsid and expression cassette optimization. Mol. Ther. Methods Clin. Dev. *32*, 101185. https://doi.org/10.1016/j.omtm.2024.101185.

25. Tenenbaum, L., Chtarto, A., Lehtonen, E., Velu, T., Brotchi, J., and Levivier, M. (2004). Recombinant AAV-mediated gene delivery to the central nervous system. J. Gene Med. *6*, S212–S222. https://doi.org/10.1002/jgm.506.

26. Kawabata, H., Konno, A., Matsuzaki, Y., and Hirai, H. (2023). A blood-brain barrier-penetrating AAV2 mutant created by a brain microvasculature endothelial cell-targeted AAV2 variant. Mol. Ther. Methods Clin. Dev. *29*, 81–92. https://doi.org/10.1016/j.omtm.2023.02.016.

27. Konno, A., Shinohara, Y., and Hirai, H. (2024). Production of Spinocerebellar Ataxia Type 3 Model Mice by Intravenous Injection of AAV-PHP.B Vectors. Int. J. Mol. Sci. *25*, 7205. https://doi.org/10.3390/ijms25137205.

28. Radhiyanti, P.T., Konno, A., Matsuzaki, Y., and Hirai, H. (2021). Comparative study of neuron-specific promoters in mouse brain transduced by intravenously administered AAV-PHP.eB. Neurosci. Lett. *756*, 135956. https://doi.org/10.1016/j.neulet.2021.135956.

29. Chuapoco, M.R., Flytzanis, N.C., Goeden, N., Christopher Octeau, J., Roxas, K.M., Chan, K.Y., Scherrer, J., Winchester, J., Blackburn, R.J., Campos, L.J., et al. (2023). Adeno-associated viral vectors for functional intravenous gene transfer throughout the non-human primate brain. Nat. Nanotechnol. *18*, 1241–1251. https://doi.org/10.1038/s41565-023-01419-x.

30. Goertsen, D., Flytzanis, N.C., Goeden, N., Chuapoco, M.R., Cummins, A., Chen, Y., Fan, Y., Zhang, Q., Sharma, J., Duan, Y., et al. (2022). AAV capsid variants with brain-wide transgene expression and decreased liver targeting after intravenous delivery in mouse and marmoset. Nat. Neurosci. *25*, 106–115. https://doi.org/10.1038/s41593-021-00969-4.

31. Yao, Y., Wang, J., Liu, Y., Qu, Y., Wang, K., Zhang, Y., Chang, Y., Yang, Z., Wan, J., Liu, J., et al. (2022). Variants of the adeno-associated virus serotype 9 with enhanced penetration of the blood-brain barrier in rodents and primates. Nat. Biomed. Eng. *6*, 1257–1271. https://doi.org/10.1038/s41551-022-00938-7.

32. Hanlon, K.S., Meltzer, J.C., Buzhdygan, T., Cheng, M.J., Sena-Esteves, M., Bennett, R.E., Sullivan, T.P., Razmpour, R., Gong, Y., Ng, C., et al. (2019). Selection of an Efficient AAV Vector for Robust CNS Transgene Expression. Mol. Ther. Methods Clin. Dev. *15*, 320–332. https://doi.org/10.1016/j.omtm.2019.10.007.

33. Matsuzaki, Y., Konno, A., Mochizuki, R., Shinohara, Y., Nitta, K., Okada, Y., and Hirai, H. (2018). Intravenous administration of the adeno-associated virus-PHP.B capsid fails to upregulate transduction efficiency in the marmoset brain. Neurosci. Lett. *665*, 182–188. https://doi.org/10.1016/j.neulet.2017.11.049.

34. Shinohara, Y., Konno, A., Takahashi, N., Matsuzaki, Y., Kishi, S., and Hirai, H. (2016). Viral Vector-Based Dissection of Marmoset GFAP Promoter in Mouse and Marmoset Brains. PLoS One *11*, e0162023. https://doi.org/10.1371/journal.pone.0162023.

35. Boshart, M., Weber, F., Jahn, G., Dorsch-Häsler, K., Fleckenstein, B., and Schaffner, W. (1985). A very strong enhancer is located upstream of an immediate early gene of human cytomegalovirus. Cell *41*, 521–530. https://doi.org/10.1016/s0092-8674(85)80025-8.

36. Haustein, M.D., Kracun, S., Lu, X.H., Shih, T., Jackson-Weaver, O., Tong, X., Xu, J., Yang, X.W., O'Dell, T.J., Marvin, J.S., et al. (2014). Conditions and constraints for astrocyte calcium signaling in the hippocampal mossy fiber pathway. Neuron *82*, 413–429. https://doi.org/10.1016/j.neuron.2014.02.041.

37. Challis, R.C., Ravindra Kumar, S., Chan, K.Y., Challis, C., Beadle, K., Jang, M.J., Kim, H.M., Rajendran, P.S., Tompkins, J.D., Shivkumar, K., et al. (2019). Systemic AAV vectors for widespread and targeted gene delivery in rodents. Nat. Protoc. *14*, 379–414. https://doi.org/10.1038/s41596-018-0097-3.

38. Konno, A., and Hirai, H. (2020). Efficient whole brain transduction by systemic infusion of minimally purified AAV-PHP.eB. J. Neurosci. Methods *346*, 108914. https://doi.org/10.1016/j.jneumeth.2020.108914.

39. Sohn, J., Takahashi, M., Okamoto, S., Ishida, Y., Furuta, T., and Hioki, H. (2017). A single vector platform for high-level gene transduction of central neurons: Adeno-associated virus vector equipped with the tet-off system. PLoS One *12*, e0169611. https://doi.org/10.1371/journal.pone.0169611.

40. Takahashi, M., Ishida, Y., Kataoka, N., Nakamura, K., and Hioki, H. (2021). Efficient labeling of neurons and identification of postsynaptic sites using adeno-associated virus vector. In Receptor and Ion Channel Detection in the Brain, R. Lujan and F. Ciruela, eds. (Springer US), pp. 323–341. https://doi.org/10.1007/978-1-0716-1522-5_22.